Author Manuscript

Author Manuscript

Author Manuscript

Author Manuscript

HHS Public Access

Author manuscript

Biochem Biophys Res Commun. Author manuscript; available in PMC 2017 October 28.

Published in final edited form as:

Biochem Biophys Res Commun. 2016 October 28; 479(4): 875–880. doi:10.1016/j.bbrc.2016.09.114.

Gene expression profiling of brain samples from patients with Lewy body dementia

Maciej Pietrzak[1,2], **Audrey Papp**[1], **Amanda Curtis**[1], **Samuel K. Handelman**[3], **Maria Kataki**[4], **Douglas W. Scharre**[4], **Grzegorz Rempala**[2,5], and **Wolfgang Sadee**[1]

[1]Center for Pharmacogenomics, Department of Cancer Biology and Genetics, College of Medicine, The Ohio State University Columbus, OH, USA

[2]Mathematical Biosciences Institute, The Ohio State University, Columbus, OH, USA

[3]Department of Obstetrics and Gynecology, Wayne State University, Detroit MI, USA

[4]Department of Neurology, College of Medicine, The Ohio State University, Columbus OH, USA

[5]Division of Biostatistics, College of Public Health, The Ohio State University, Columbus, OH, USA

Abstract

Dementia with Lewy Bodies (DLB) is the second most common neurodegenerative disorder in the elderly. The development and progression of DLB remain unclear. In this study we used next generation sequencing to assess RNA expression profiles and cellular processes associated with DLB in the anterior cingulate cortex, a brain region affected by DLB pathology. The expression measurements were made in autopsy brain tissues from 8 DLB subjects and 10 age-matched controls using AmpliSeq technology with ion torrent sequencing. The analysis of RNA expression profiles revealed 490 differentially expressed genes, among which 367 genes were down-regulated and 123 were up-regulated. Functional enrichment analysis of genes differentially expressed in DLB indicated downregulation of genes associated with myelination, neurogenesis, and regulation of nervous system development. miRNA binding sites enriched in these mRNAs yielded a list of candidate miRNAs participating in DLB pathophysiology. Our study provides a comprehensive picture of gene expression landscape in DLB, identifying key cellular processes associated with DLB pathology.

Keywords

Neurodegeneration; Dementia with Lewy bodies; anterior cingulate cortex; gene expression profiling; RNA profiling by amplicon sequencing

Corresponding Author: Wolfgang Sadee, Wolfgang.Sadee@osumc.edu.

Publisher's Disclaimer: This is a PDF file of an unedited manuscript that has been accepted for publication. As a service to our customers we are providing this early version of the manuscript. The manuscript will undergo copyediting, typesetting, and review of the resulting proof before it is published in its final citable form. Please note that during the production process errors may be discovered which could affect the content, and all legal disclaimers that apply to the journal pertain.

Author Manuscript Author Manuscript Author Manuscript Author Manuscript

Introduction

Dementia with Lewy bodies (DLB) is the second most common neurodegenerative disorder after Alzheimer's disease (AD) in people older than 65 years [1, 2]. It is characterized by cognitive decline, Parkinsonism, visual hallucinations, cognitive/behavioral fluctuations, and dream-enactment behaviors [3, 4]. Heitz *et al.* revealed an association between impairment of anterior cingulate cortex (ACC) and visual hallucinations in DLB patients [6]. DLB is marked by Lewy body (LB) deposition in cortical regions including ACC and entorhinal cortex, in correlation with cognitive decline [5]. Abnormal accumulation of α-synuclein protein forms LBs in neurons (round eosinophilic hyaline inclusions), leading to dystrophy of axons and dendrites, and Lewy neuritis (LNs) with loss of neurons, mainly cholinergic and dopaminergic [7]. Despite extensive studies of the role of α-synuclein in DLB pathology, the mechanisms leading to accumulation of LD and LN remains poorly understood [8].

Transcriptome profiling is a powerful approach for identification of gene expression patterns characteristic of diseases. So far, to the best of our knowledge, DLB-associated gene expression profiles have yet to be published. In this study we applied next generation sequencing technology to assess RNA expression profiles in anterior cingulate cortex autopsy tissues from DLB subjects and age-matched controls lacking a diagnosis of neurodegenerative disorders, to identify genes and cellular processes associated with DLB pathology.

Material and methods

Postmortem human brain specimens

Human brain tissue for this study was obtained from the Buckeye Brain Bank at the Wexner Ohio State Medical Center (DLB cases) and the Miami Brain Endowment Bank (University of Miami, Miami, FL), maintained under respective IRB protocols. DLB diagnosis was confirmed by basic clinical and neuropathological analyses. We analyzed eight anterior cingulate cortex samples obtained from subjects suffering DLB and from ten age-matched controls lacking a diagnosis of neurodegenerative disorders.

RNA isolation

Initial RNA extraction was performed using TRIzol Reagent (Ambion, Austin, TX), according to the manufacturer's instructions. Briefly, 100 mg of frozen brain tissue was homogenized in Trizol and then phase separated with chloroform. The upper aqueous phase was transferred to a new tube, and RNA was precipitated by adding isopropyl alcohol. The RNA precipitate was pelleted by centrifugation, and dissolved in 50μl of RNase free water. RNA was further purified using the SpinSmart RNA purification kit (Denville Scientific) and treated with DNase according to the manufacturer's protocol. Enzyme treated RNA was washed to remove degraded deoxynucleic acids and eluted in RNase free water. RNA concentration was measured using the Qubit RNA assay (ThermoFisher, Carlsbad, CA) and RNA integrity was assessed by Bioanalyzer (Agilent, Santa Clara, CA), as described in [9].

Author Manuscript Author Manuscript Author Manuscript Author Manuscript

Library preparation and amplicon sequencing

The Ion AmpliSeq Transcriptome Human Gene Expression Kit (ThermoFisher) enables the simultaneous measurement of the expression levels of over 20,000 human genes in a single assay. Reverse transcription was performed on 10 ng of the prepared brain total RNA using the AmpliSeq Whole Transcriptome primers with the included SuperScript VILO cDNA Synthesis kit. The resulting cDNA was amplified for 12 cycles using Ion AmpliSeq primers and technology to accurately maintain expression levels of all genes. Barcoded adapters were added and ligated to individual reactions, and the resulting libraries were purified using Agencourt AMPure XP reagents (Beckman Coulter, LaBrea, CA) without any additional amplification. The limited number of PCR cycles reduces biased amplification of highly abundant molecules and also reduces dropout of low abundance transcripts, as well as minimizes the confounding effect of undesirable PCR duplicates produced by higher cycle numbers. This facilitates a precise and sensitive linear range of measurement of gene expression over 6 orders of magnitude.

The purified library concentrations were determined by quantitative real time PCR with Ion Torrent adapter primers and SYBR Green detection. The quantified barcoded libraries were diluted to 100 pM. All libraries were combined and pooled in equal amounts for emulsion PCR on the Ion OneTouch 2 instrument. The OneTouch 2 system uses emulsion PCR to produce templated Ion Sphere Particles used for Ion Torrent semiconductor sequencing. Templated libraries were sequenced with the Ion Proton sequencer, using Ion PITM Sequencing 200 Kit v2 reagents, on Ion PITM Chips.

Gene expression analysis

AmpliSeq sequencing data were analyzed using the Ion Torrent Mapping Alignment Program (TMAP), which is optimized for aligning the raw sequencing reads against reference sequences targeted by the AmpliSeq kit primers. To achieve both specificity and sensitivity, TMAP implements a two-stage mapping approach, using four alignment algorithms, BWA-short and long, SSAHA, and Super-maximal Exact Matching. This is followed by the Smith Waterman algorithm to find the final best mapping [10–13]. Differentially expressed genes (DEGs) were determined using the R package edgeR [14], as described in [15]. The package is available from Bioconductor. RNAs with less than fifty read counts on average across all samples were excluded from further analysis. DEGs were selected based on p-value and log2 fold change (log2FC). Pairwise analysis of RNA profile similarity was performed using I-Index, which was calculated for each pair of samples [16]. The pairwise similarity matrix was used for hierarchical clustering as described in [15]. Analysis was performed using the R package “divo”, which is available for download in the CRAN repository (https://cran.r-project.org/web/packages/divo).

Functional annotation analysis

Protein-coding RNAs selected for analysis were significantly differentially expressed genes between DLB subjects and age-matched controls based on p-value and Log2FC. We used the ToppFun application of ToppGene [17] for the identification of enriched functional categories among DEGs in DLB brains. We also assessed enrichment of biological processes in gene ontology (GO) and Kyoto Encyclopedia of Genes and Genomes (KEGG) pathways.

Author Manuscript Author Manuscript Author Manuscript Author Manuscript

Bonferroni-corrected p-values for the statistical tests of functional enrichment of less than 0.05 were considered statistically significant. Identification of putative common miRNA regulators was performed using miRTarbase, TargetScan, and MicroRNA.org [18–20].

Results

RNA was isolated from anterior cingulate cortex, a brain region affecting cognitive outcomes in DLB [5], from 8 DLB subjects and 10 age-matched controls. To assess gene expression profiles, we applied an amplicon sequencing approach using 20812 probes sets specific to human mRNA, yielding more than 3,900,000 mapped reads per sample with alignment rates > 92%. The outcomes of AmpliSeq analysis are highly reproducible [21]; the results obtained by us, and other groups, in a number of projects renders Ampliseq RNA profiling well suitable for large-scale screening of DEGs, guiding subsequent targeted approaches.

For analysis of differential gene expression between DLB subjects and controls we included signals from > 9300 amplicons with mean mapped reads higher than 50 reads across all subjects. Differential gene expression analysis revealed 136 DEGs at a false discovery rate of 5% (Figure 1), of which 18 were at higher expression in DLB and 118 were at lower expression. To cast a wider net, we selected genes showing DE with twofold difference and a p-value < 0.01. The results, presented in a volcano plot (Figure 1), illustrate a trend towards more DEGs being down-regulated. The 10 most strongly up- and downregulated genes in DLB subjects are listed in Tables 1A and 1B. The top upregulated genes were as follows: thyroid hormone transporter transthyretin (*TTR*; FC = 9.4; FDR ≤ 0.02); zinc finger transcriptional repressor scratch family zinc finger 1 (*SCRT1*; FC = 2.4; FDR ≤ 0.04) and metallothionein 1H (*MT1H*; FC = 3.36; FDR ≤ 0.05). Among top downregulated genes we identified carbohydrate transmembrane transporter transmembrane protein 144 (*TMEM144*; FC = 0.14; FDR ≤ 0.006), CD9 molecule (*CD9*; FC = 0.3; FDR ≤ 0.0019), and myelin regulatory factor (*MYRF*; FC = 0.23; FDR ≤ 0.006). The expression of DEGs and those showing a DE trend (Supplementary Table S1) is presented in Figure 2A. Hierarchical clustering analysis of gene expression revealed coexpression of gene groups indicated by reduction of Euclidian distances between genes (Figure 2A). To assess overall differences of RNA expression profiles between DLB subjects and controls, we assessed pairwise similarity of the profiles for each pair of samples using the I-Index (Figure 2B). Hierarchical clustering revealed a lack of DLB-specific sample clustering, and the distance between samples was small, suggesting specificity of observed differences of gene expression.

Functional enrichment analysis of DEG in DLB (minimum 2-fold change and p-value < 0.01; 490 genes) revealed 20 biological processes including axon ensheathment (16 genes; p = 3.91E-9), myelination (15 genes; p = 4.09E-8), neurogenesis (48 genes, p = 7.48E-4), and regulation of nervous system development (26 genes; p = 4.62E-2) (Table 2). Among genes in the enriched GO categories: myelination, neurogenesis, and regulation of gliogenesis, 5 genes were upregulated in DLB while 45 were downregulated. Upregulated genes included adrenomedullin (*ADM*), nuclear receptor subfamily 2, group F, member 1 (*NR2F1*), and vascular endothelial growth factor A (*VEGFA*). Downregulated genes included apoptosis-

Author Manuscript Author Manuscript Author Manuscript Author Manuscript

associated tyrosine kinase (*AATK*), myelin associated glycoprotein (*MAG*), and transferrin (*TF*) (Figure 3).

The analysis of putative targets of miRNAs in the pool of DEGs in DLB revealed 14 candidate miRNAs that can potentially regulate pools of 30 to 74 genes (FDR< 4.1E-2) (Figure 4 and Table S2). For example, 35 DEGs, including cyclin-dependent kinase inhibitor 1C (p57, Kip2) (*CDKN1C*), transmembrane protein 144 (*TMEM144*), and myelin oligodendrocyte glycoprotein (*MOG*), are putative targets of miR-25. DEG targets of miR-9 (26 DE genes; FDR ≤ 7.708E-3) include myosin ID (*MYO1D*), presenilin 1 (*PSEN1*), apoptosis-associated tyrosine kinase (*AATK*), and ubiquitin protein ligase E3A (*UBE3A*), while miR-124 targets (37 DE genes; FDR ≤ 2.191E-4) include dicer 1 ribonuclease III (*DICER1*), microtubule associated protein 7 (*MAP7*) and semaphorin 6A (*SEMA6A*) (Figure 4 and Table S2).

Discussion

While specific biological processes leading to neurodegeneration in patients with dementia with Lewy bodies have been studied [2], a comprehensive analysis of the gene expression landscape was lacking. This pilot study with 8 DLB cases and 10 controls demonstrates differences in gene expression profiles in a brain region affected by DLB pathology, the anterior cingulate cortex. Measuring gene expression using the AmpliSeq approach – a method of high sensitivity and reproducibility [21], facilitated detection of 136 genes (FDR ≤ 0.05) differently expressed in DLB, even with a relatively small sample size. For a less stringent broader analysis, we included genes showing a DE trend, potentially relevant to DLB pathology.

A majority of significant DE genes were found to be downregulated, possibly a result of loss of cholinergic and dopaminergic neurons in DLB-affected brains. On the other hand, reduced activity of specific pathways could also point to underlying processes leading to DLB. Gene ontology analysis revealed numerous genes downregulated in DLB brains involved in neurogenesis: 48 genes (Bonferroni corrected p-value 7.475E-4) including transferrin (*TF*), cyclin-dependent kinase inhibitor 1C (*CDKN1C*), and presenilin 1 (*PSEN1*). On the other hand, genes such as adrenomedullin (*ADM*), EPH receptor B1 (*EPHB1*), and vascular endothelial growth factor A (*VEGFA*) were upregulated, suggesting that loss of neurons may not be the main cause of these changes. Another large group of downregulated genes is associated with myelination, including myelin associated glycoprotein (*MAG*), contactin 2 (*CNTN2*), and dicer 1, ribonuclease type III (*DICER1*), (Bonferroni corrected p-value 4.088E-8). Previous evidence is lacking for a role of demyelination in DLB pathology, affecting axonal degeneration and subsequent neuronal loss [22]. Other processes identified by enrichment analysis include CNS development, cytoskeleton organization, and blood vessel morphogenesis. Whether these processes contribute to DLB pathology or result from it remains to be clarified.

Gene expression profiling of samples with advanced neurodegeneration might reveal general gene expression differences not specific to any particular disease. To test whether differences in gene expression are DLB-specific, we compared our results with studies describing other

Author Manuscript Author Manuscript Author Manuscript Author Manuscript

neurodegenerative disorders. Analysis of gene expression profiles in DLB revealed 46 DE genes that were upregulated in brain samples with Alzheimer's disease pathology [23]. Only four of these genes were also upregulated in DLB: cytokine receptor-like factor 1 (*CRLF1*) – a member of the cytokine type I receptor family that forms a protein complex promoting survival of neuronal cells; F-box protein 2 (*FBXO2*) – the F-box protein family member similar to rat nfb42 which is enriched in the nervous system and plays a role in maintaining neurons in a postmitotic state; nuclear receptor subfamily 2 group F member 1 (*NR2F1*) – important paralog of *RXRG*, and metallothionein 1H (*MT1H*) – a member of class 1 metallothioneins, involved in detoxification and maintaining the homeostasis of heavy metals [24], control of oxidative stress [25]. Conversely, 42 genes showing increased expression in AD, such as: ATP-binding cassette transporter 2 (*ABCA2*), cyclin-dependent kinase inhibitor 1C (*CDKN1C*), double-stranded RNA-specific endoribonuclease (*DICER1*), microtubule-associated protein 7 (*MAP7*), semaphorin 3B (*SEMA3B*), and tubulin alpha 1a (*TUBA1A*), were downregulated in DLB (Table S1). The differences of direction of these expression changes between DLB and AD could have resulted from the different etiology of synucleinopathies and tauopathies [26]. Two genes upregulated in DLB ACC tissues had also been reported upregulated in Huntington's disease (HD): metallothionein 1G (*MT1G*) in motor cortex and nuclear receptor subfamily 1 Group D Member 1 (*NR1D1*) in cerebellum [27]. Similarly, two genes downregulated in ACC in DLB brains were also found downregulated in HD: engulfment and cell motility 1 (*ELMO1*) in caudate nucleus and *PSEN1* in motor cortex [27]. Conversely, several genes downregulated in DLB are upregulated in HD brain: serpin family A member 3 (*SERPINA3*), apelin receptor (*AGTRL1*), serum/glucocorticoid regulated kinase (*SGK*), and aquaporin 1 (*AQP1*) [27, 28]. The relatively limited overlap of gene expression profiles between DLB and other neurodegenerative disorders suggests that a portion of alternations observed in our study is not a general hallmark of neurodegeneration but rather represents gene expression changes that regulate disease-specific processes providing insight into DLB etiology.

The identified DE genes relevant to DLB enable us to deduce possible roles for miRNAs interacting with these mRNAs. miRNAs play a substantial role in the regulation of gene expression in the brain [29–31]. Approximately 70% of experimentally identified miRNAs are expressed in the human nervous system, orchestrating multiple cellular processes by posttranscriptional regulation of numerous genes [32]. To identify putative regulatory miRNA that might contribute to DLB pathology, we screened the mRNAs of DEGs for putative miRNA binding sites. The analysis revealed 14 candidate miRNA that regulate sets of genes containing 30 – 74 DEGs. Among candidate miRNAs, we identified miR-9 and miR-124 – crucial for regulation of adult neurogenesis [33, 34]. Moreover miR-124 plays a critical role in CNS stress response, regulation of synaptic plasticity and memory, and neurodegenerative disorders such as AD and Parkinson's disease [35]. These findings provide a guide for further studies on the role of miRNAs in molecular mechanisms underlying neurodegeneration and specifically DLB.

In summary, RNA transcriptome analysis of brains affected by DLB revealed disease-specific gene expression profile differences. Enrichment analysis indicated downregulation of groups of genes associated with myelination and neurogenesis in DLB. miRNA binding

Author Manuscript Author Manuscript Author Manuscript Author Manuscript

sites enriched in DE mRNAs yielded a list of candidate miRNAs participating in DLB pathophysiology, guiding future studies.

Supplementary Material

Refer to Web version on PubMed Central for supplementary material.

Acknowledgments

This work was supported by NIH grants: U01 NIGMS GM092655 to WS, R01 CA152158 to GR and the Mangurian Foundation. The authors would like to thank Ms. Gloria Smith for excellent technical assistance.

References

1. Buracchio T, Arvanitakis Z, Gorbien M. Dementia with Lewy bodies: current concepts. Dement Geriatr Cogn Disord. 2005; 20:306–320. [PubMed: 16174977]
2. McKeith I, Mintzer J, Aarsland D, Burn D, Chiu H, Cohen-Mansfield J, Dickson D, Dubois B, Duda JE, Feldman H, Gauthier S, Halliday G, Lawlor B, Lippa C, Lopez OL, Carlos Machado J, O'Brien J, Playfer J, Reid W. D.L.B. International Psychogeriatric Association Expert Meeting on, Dementia with Lewy bodies. Lancet Neurol. 2004; 3:19–28. [PubMed: 14693108]
3. Armstrong RA. Visual signs and symptoms of dementia with Lewy bodies. Clin Exp Optom. 2012; 95:621–630. [PubMed: 22812926]
4. Pao WC, Boeve BF, Ferman TJ, Lin SC, Smith GE, Knopman DS, Graff-Radford NR, Petersen RC, Parisi JE, Dickson DW, Silber MH. Polysomnographic findings in dementia with Lewy bodies. Neurologist. 2013; 19:1–6. [PubMed: 23269098]
5. Kovari E, Gold G, Herrmann FR, Canuto A, Hof PR, Bouras C, Giannakopoulos P. Lewy body densities in the entorhinal and anterior cingulate cortex predict cognitive deficits in Parkinson's disease. Acta Neuropathol. 2003; 106:83–88. [PubMed: 12687392]
6. Heitz C, Noblet V, Cretin B, Philippi N, Kremer L, Stackfleth M, Hubele F, Armspach JP, Namer I, Blanc F. Neural correlates of visual hallucinations in dementia with Lewy bodies. Alzheimers Res Ther. 2015; 7:6. [PubMed: 25717349]
7. Nordström E, Kasrayan A, Ekberg M, Sundquist VS, Lannfelt L, Holmquist M. Protofibril-binding antibodies and their use in therapeutic and diagnostic methods for Parkinson's disease, dementia with lewy bodies and other α-synucleinopathies. Google Patents. 2014
8. Mukaetova-Ladinska EB, Andras A, Milne J, Abdel-All Z, Borr I, Jaros E, Perry RH, Honer WG, Cleghorn A, Doherty J, McIntosh G, Perry EK, Kalaria RN, McKeith IG. Synaptic proteins and choline acetyltransferase loss in visual cortex in dementia with Lewy bodies. J Neuropathol Exp Neurol. 2013; 72:53–60. [PubMed: 23242284]
9. Webb A, Papp AC, Curtis A, Newman LC, Pietrzak M, Seweryn M, Handelman SK, Rempala GA, Wang D, Graziosa E, Tyndale RF, Lerman C, Kelsoe JR, Mash DC, Sadee W. RNA sequencing of transcriptomes in human brain regions: protein-coding and non-coding RNAs, isoforms and alleles. BMC Genomics. 2015; 16:990. [PubMed: 26597164]
10. Li H, Durbin R. Fast and accurate short read alignment with Burrows-Wheeler transform. Bioinformatics. 2009; 25:1754–1760. [PubMed: 19451168]
11. Li H, Durbin R. Fast and accurate long-read alignment with Burrows-Wheeler transform. Bioinformatics. 2010; 26:589–595. [PubMed: 20080505]
12. Ning Z, Cox AJ, Mullikin JC. SSAHA: a fast search method for large DNA databases. Genome Res. 2001; 11:1725–1729. [PubMed: 11591649]
13. Li H. Exploring single-sample SNP and INDEL calling with whole-genome de novo assembly. Bioinformatics. 2012; 28:1838–1844. [PubMed: 22569178]
14. Robinson MD, McCarthy DJ, Smyth GK. edgeR: a Bioconductor package for differential expression analysis of digital gene expression data. Bioinformatics. 2010; 26:139–140. [PubMed: 19910308]

Author Manuscript Author Manuscript Author Manuscript Author Manuscript

15. Mascarenhas R, Pietrzak M, Smith RM, Webb A, Wang D, Papp AC, Pinsonneault JK, Seweryn M, Rempala G, Sadee W. Allele-Selective Transcriptome Recruitment to Polysomes Primed for Translation: Protein-Coding and Noncoding RNAs, and RNA Isoforms. PLoS One. 2015; 10:e0136798. [PubMed: 26331722]
16. Rempala GA, Seweryn M. Methods for diversity and overlap analysis in T-cell receptor populations. J Math Biol. 2013; 67:1339–1368. [PubMed: 23007599]
17. Chen J, Bardes EE, Aronow BJ, Jegga AG. ToppGene Suite for gene list enrichment analysis and candidate gene prioritization. Nucleic Acids Res. 2009; 37:W305–W311. [PubMed: 19465376]
18. Chou CH, Chang NW, Shrestha S, Hsu SD, Lin YL, Lee WH, Yang CD, Hong HC, Wei TY, Tu SJ, Tsai TR, Ho SY, Jian TY, Wu HY, Chen PR, Lin NC, Huang HT, Yang TL, Pai CY, Tai CS, Chen WL, Huang CY, Liu CC, Weng SL, Liao KW, Hsu WL, Huang HD. miRTarBase 2016: updates to the experimentally validated miRNA-target interactions database. Nucleic Acids Res. 2016; 44:D239–D247. [PubMed: 26590260]
19. Lewis BP, Burge CB, Bartel DP. Conserved seed pairing, often flanked by adenosines, indicates that thousands of human genes are microRNA targets. Cell. 2005; 120:15–20. [PubMed: 15652477]
20. Betel D, Wilson M, Gabow A, Marks DS, Sander C. The microRNA.org resource: targets and expression. Nucleic Acids Res. 2008; 36:D149–D153. [PubMed: 18158296]
21. Li W, Turner A, Aggarwal P, Matter A, Storvick E, Arnett DK, Broeckel U. Comprehensive evaluation of AmpliSeq transcriptome, a novel targeted whole transcriptome RNA sequencing methodology for global gene expression analysis. BMC Genomics. 2015; 16:1069. [PubMed: 26673413]
22. Love S. Demyelinating diseases. J Clin Pathol. 2006; 59:1151–1159. [PubMed: 17071802]
23. Blalock EM, Geddes JW, Chen KC, Porter NM, Markesbery WR, Landfield PW. Incipient Alzheimer's disease: microarray correlation analyses reveal major transcriptional and tumor suppressor responses. Proc Natl Acad Sci U S A. 2004; 101:2173–2178. [PubMed: 14769913]
24. Hamer DH. Metallothionein. Annu Rev Biochem. 1986; 55:913–951. [PubMed: 3527054]
25. Kumari MV, Hiramatsu M, Ebadi M. Free radical scavenging actions of metallothionein isoforms I and II. Free Radic Res. 1998; 29:93–101. [PubMed: 9790511]
26. Hickey C, Chisholm T, Passmore MJ, O'Brien JD, Johnston J. Differentiating the dementias. Revisiting synucleinopathies and tauopathies. Curr Alzheimer Res. 2008; 5:52–60. [PubMed: 18288932]
27. Hodges A, Strand AD, Aragaki AK, Kuhn A, Sengstag T, Hughes G, Elliston LA, Hartog C, Goldstein DR, Thu D, Hollingsworth ZR, Collin F, Synek B, Holmans PA, Young AB, Wexler NS, Delorenzi M, Kooperberg C, Augood SJ, Faull RL, Olson JM, Jones L, Luthi-Carter R. Regional and cellular gene expression changes in human Huntington's disease brain. Hum Mol Genet. 2006; 15:965–977. [PubMed: 16467349]
28. Rangone H, Poizat G, Troncoso J, Ross CA, MacDonald ME, Saudou F, Humbert S. The serum- and glucocorticoid-induced kinase SGK inhibits mutant huntingtin-induced toxicity by phosphorylating serine 421 of huntingtin. Eur J Neurosci. 2004; 19:273–279. [PubMed: 14725621]
29. Codocedo JF, Inestrosa NC. Environmental control of microRNAs in the nervous system: Implications in plasticity and behavior. Neurosci Biobehav Rev. 2016; 60:121–138. [PubMed: 26593111]
30. Sun E, Shi Y. MicroRNAs: Small molecules with big roles in neurodevelopment and diseases. Exp Neurol. 2015; 268:46–53. [PubMed: 25128264]
31. Szafranski K, Abraham KJ, Mekhail K. Non-coding RNA in neural function, disease, and aging. Front Genet. 2015; 6:87. [PubMed: 25806046]
32. Nowak JS, Michlewski G. miRNAs in development and pathogenesis of the nervous system. Biochem Soc Trans. 2013; 41:815–820. [PubMed: 23863137]
33. Coolen M, Katz S, Bally-Cuif L. miR-9: a versatile regulator of neurogenesis. Front Cell Neurosci. 2013; 7:220. [PubMed: 24312010]
34. Cheng LC, Pastrana E, Tavazoie M, Doetsch F. miR-124 regulates adult neurogenesis in the subventricular zone stem cell niche. Nat Neurosci. 2009; 12:399–408. [PubMed: 19287386]

Author Manuscript Author Manuscript Author Manuscript Author Manuscript

35. Sun Y, Luo ZM, Guo XM, Su DF, Liu X. An updated role of microRNA-124 in central nervous system disorders: a review. Front Cell Neurosci. 2015; 9:193. [PubMed: 26041995]

Author Manuscript Author Manuscript Author Manuscript Author Manuscript

Highlights

- Transcriptome profiles are measured in DLB brain
- Differentially expressed genes are involved in myelination and neurogenesis
- DE genes share putative miRNA sites, suggesting a common regulatory role in DLB

Author Manuscript Author Manuscript Author Manuscript Author Manuscript

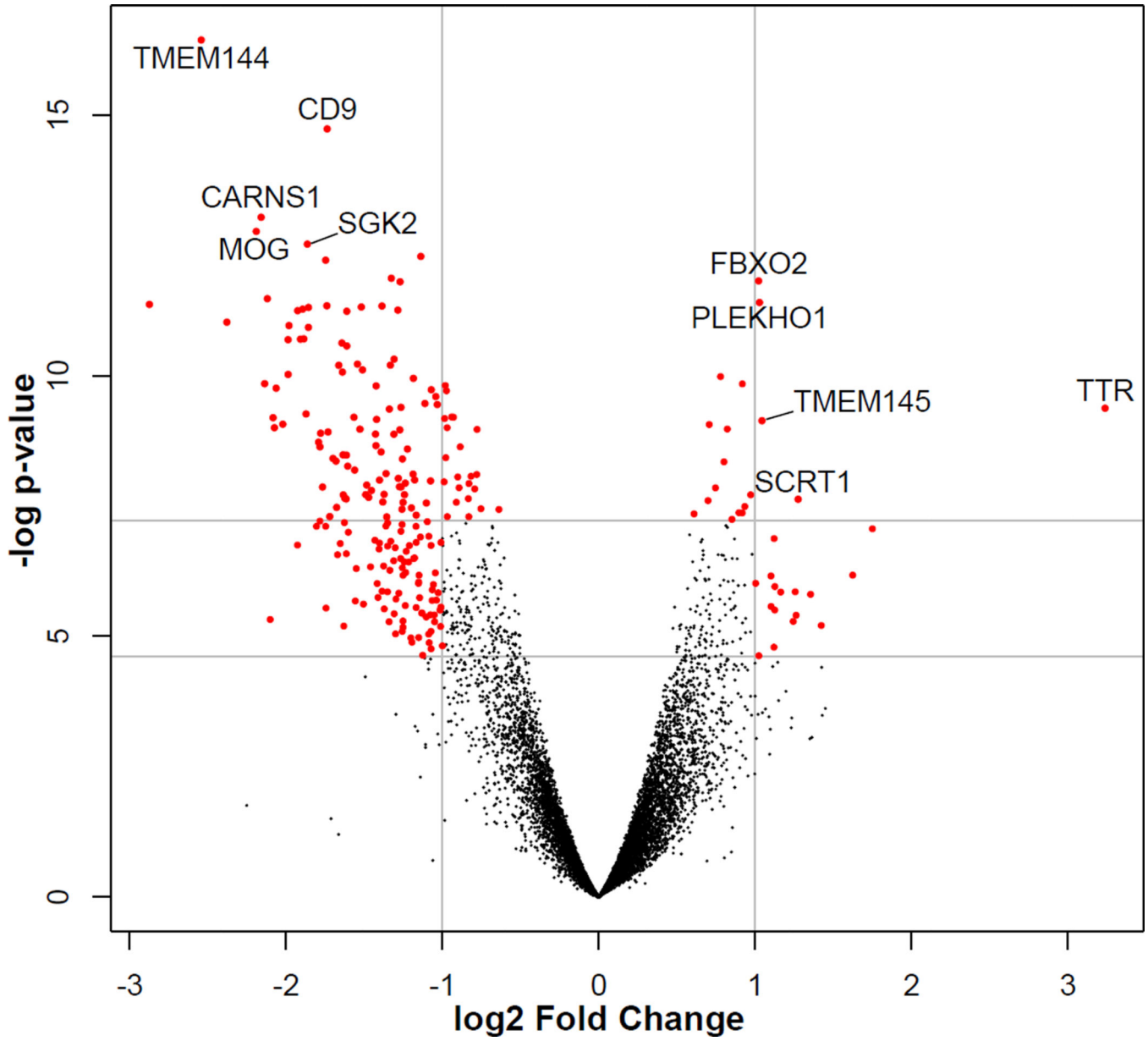

Figure 1. Gene expression differences in ACC between subjects with Lewy body dementia and age-matched controls

For each gene, log2 fold-change of expression difference is plotted on the x axis and corresponding p-value (−log) is plotted on the y axis. Genes differentially expressed (FDR < 0.05) and showing DE trend (twofold expression difference and p-value < 0.01) are marked in color red, and the top five up- and down-regulated DEGs are indicated.

Author Manuscript Author Manuscript Author Manuscript Author Manuscript

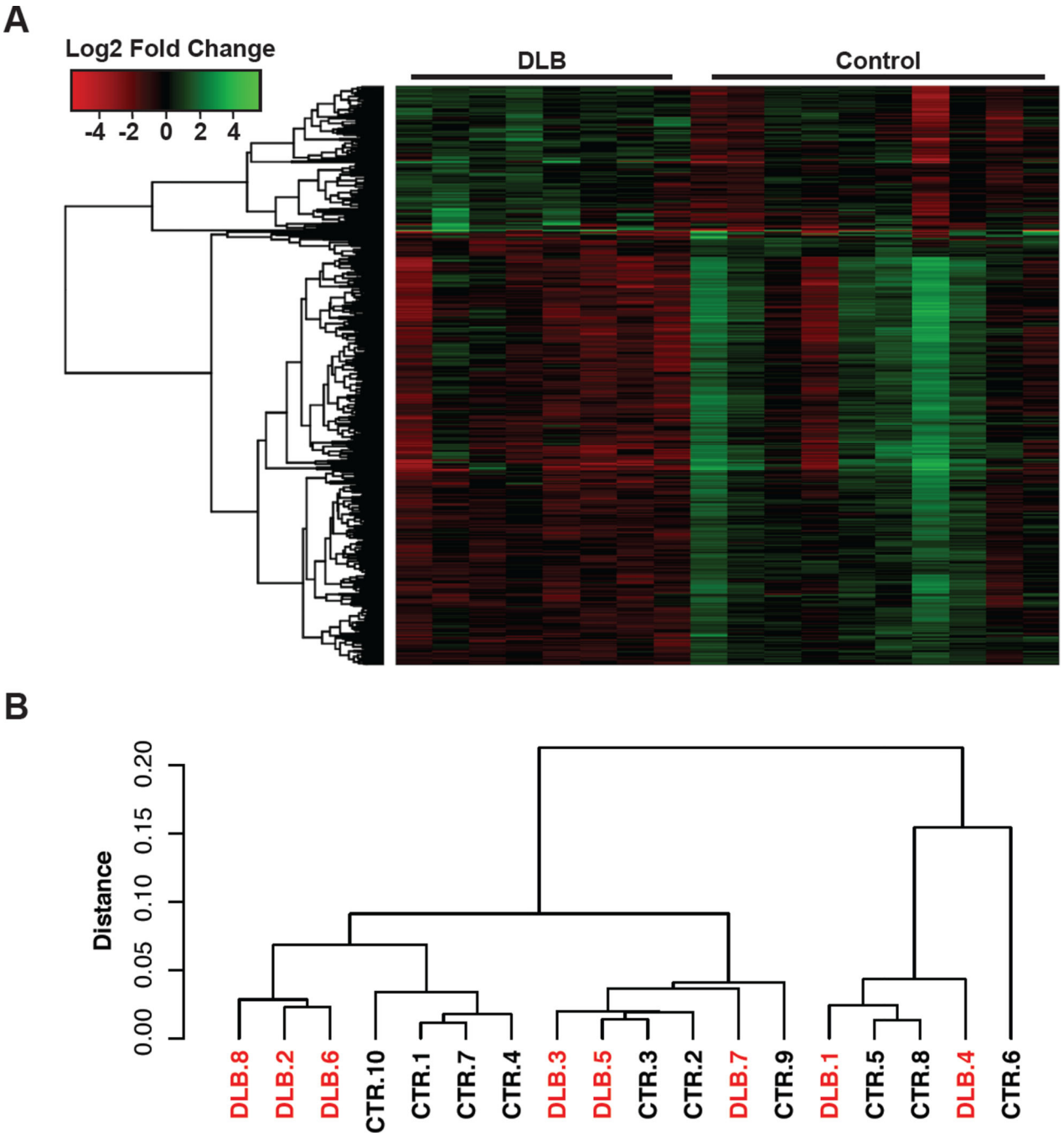

Figure 2. A. Heat map diagram of differential gene expression in ACC between dementia with Lewy bodies subjects and age-matched controls

Gene expression data obtained in AmpliSeq analysis of ACC revealed 123 genes up-regulated and 367 genes down-regulated in DLB (up-regulation is indicated by color green, down-regulation by color red) (FDR < 0.05, and genes with twofold expression difference and p-value < 0.01). Clusters of genes showing similarity of the expression patterns were identified based on Euclidian distances. **B**. Hierarchical clustering of RNA expression

profiles measured with similarity indices revealed lack of significant differences of overall expression profiles between DLB (red) and control samples (black).

Author Manuscript Author Manuscript Author Manuscript Author Manuscript

Author Manuscript Author Manuscript Author Manuscript Author Manuscript

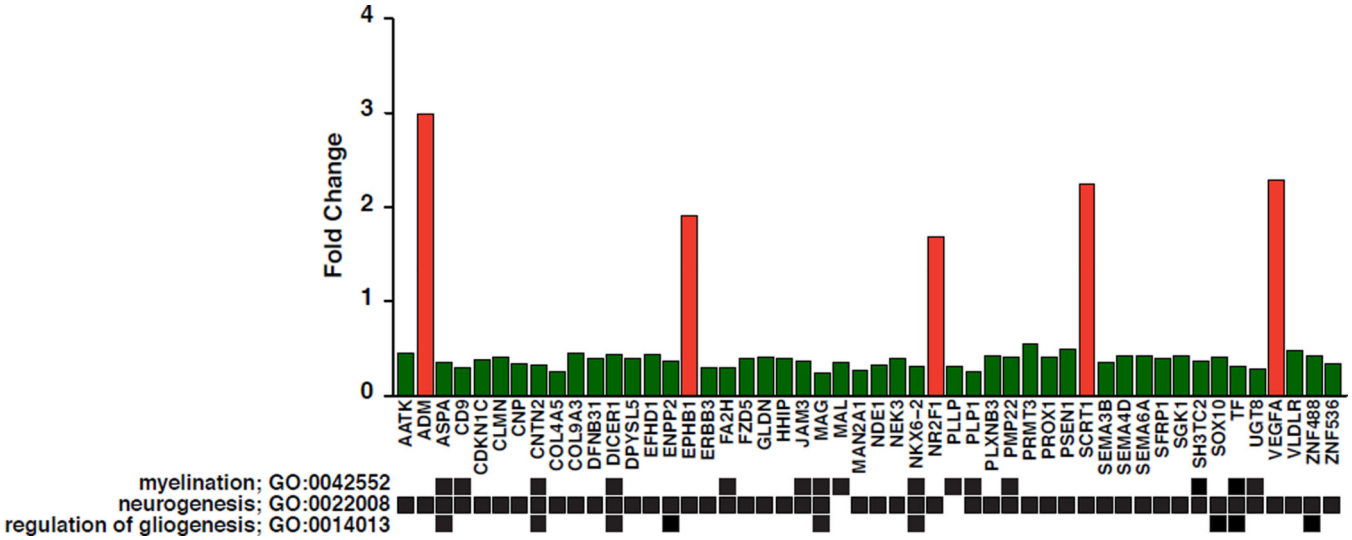

Figure 3. Gene ontology (GO) enrichment of genes differentially expressed in ACC between subject with DLB and age-matched controls

Genes identified in GO categories: Myelination, Neurogenesis, and Regulation of Gliogenesis (Bonferroni corrected p-value < 0.05); genes up-regulated in DLB are in red and down-regulated genes in green. Fold-change of expression is plotted on y axis.

Author Manuscript Author Manuscript Author Manuscript Author Manuscript

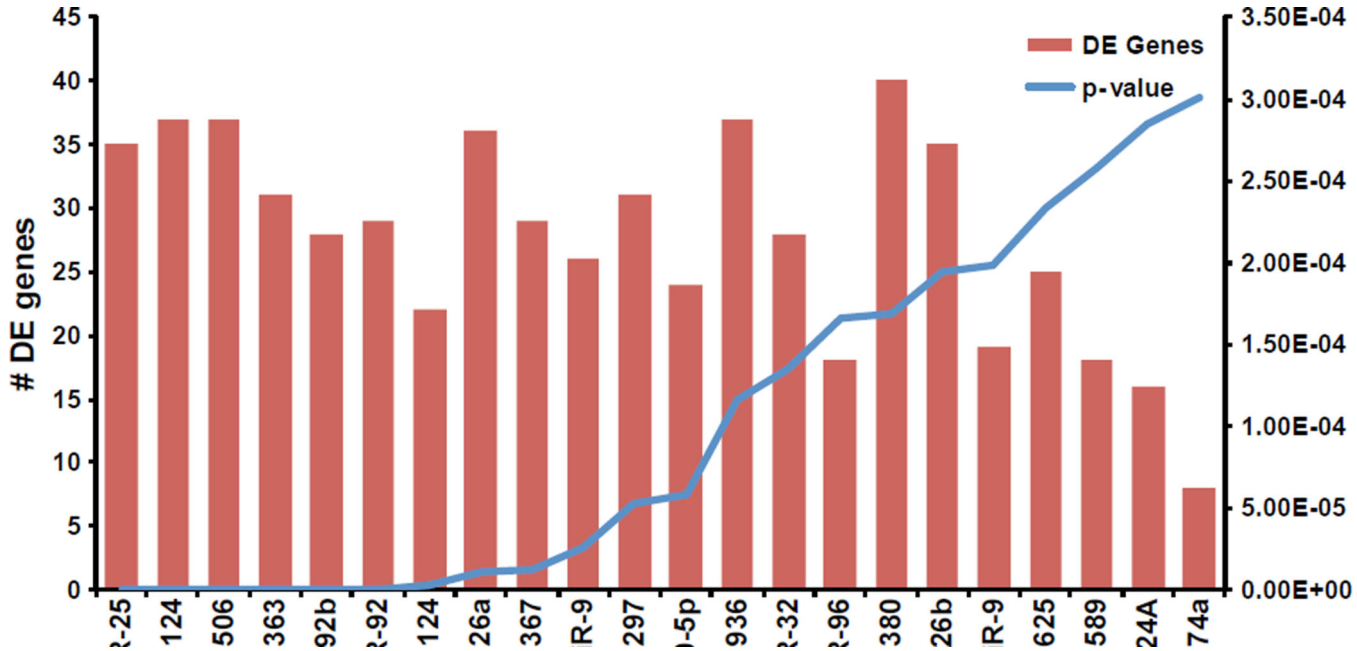

Figure 4. Identification of miRNAs targeting genes differentially expressed in ACC between subjects with dementia with Lewy bodies and age-matched controls

For DEGs in DLB we identified putative upstream regulatory miRNAs. Red bars indicate number of DE genes (read on left y axis) targeted by particular miRNA. p - values for each group are shown by the blue line (right y axis). Detailed information is provided in Table S2.

Author Manuscript Author Manuscript Author Manuscript Author Manuscript

Table 1

A. Top 10 genes upregulated in anterior cingulate cortex from DLB subject.						
Ensembl ID	**Gene**	**Gene Name**	**Position**	**log2FC**	**p-value**	**FDR**
ENSG00000118271	TTR	Transthyretin	18:31591726-31599021	3.238	8.49E-05	0.02
ENSG00000205358	MT1H	Metallothionein 1H	16:56669814-56671129	1.75	8.57E-04	0.05
ENSG00000148926	ADM	Adrenomedullin	11:10304680-10307397	1.62	2.09E-03	0.08
ENSG00000006016	CRLF1	Cytokine Receptor Like Factor 1	19:18572220-18607741	1.42	5.48E-03	0.13
ENSG00000111181	SLC6A12	Solute Carrier Family 6 Member 12	12:190077-214570	1.35	3.01E-03	0.1
ENSG00000261678	SCRT1	Scratch Family Transcriptional Repressor 1	8:144330565-144336281	1.275	4.87E-04	0.04
ENSG00000198417	MT1F	Metallothionein 1F	16:56657694-56660698	1.26	2.87E-03	0.1
ENSG00000167619	TMEM145	Transmembrane Protein 145	19:42313325-42325062	1.044	1.08E-04	0.02
ENSG00000023902	PLEKHO1	Pleckstrin Homology Domain Containing O1	1:150149183-150164720	1.028	1.12E-05	0.01
ENSG00000116661	FBXO2	F-Box Protein 2	1:11648367-11655785	1.023	7.38E-06	0.01

B. Top 10 genes downregulated in anterior cingulate cortex from DLB subjects.						
Ensembl ID	**Gene**	**Gene Name**	**Position**	**log2 FC**	**p-value**	**FDR**
ENSG00000164124	TMEM144	Transmembrane Protein 144	4:158201604-158255411	−2.54	7.26E-08	0.0007
ENSG00000010278	CD9	CD9 Molecule	12:6199715-6238271	−1.74	4.00E-07	0.002
ENSG00000204655	MOG	Myelin Oligodendrocyte Glycoprotein	6:29656981-29672372	−2.19	2.86E-06	0.006
ENSG00000172508	CARNS1	Carnosine Synthase 1	11:67414968-67425607	−2.16	2.18E-06	0.006
ENSG00000124920	MYRF	Myelin Regulatory Factor	11:61752642-61788518	−2.12	1.04E-05	0.006
ENSG00000101049	SGK2	SGK2, Serine/Threonine Kinase 2	20:43558968-43588237	−1.86	3.65E-06	0.006
ENSG00000066322	ELOVL1	ELOVL Fatty Acid Elongase 1	1:43363397-43368074	−1.75	4.96E-06	0.006
ENSG00000130150	MOSPD2	Motile Sperm Domain Containing 2	X:14873441-14922327	−1.33	7.01E-06	0.006
ENSG00000158411	MITD1	Microtubule Interacting And Trafficking Domain Containing 1	2:99161427-99181058	−1.27	7.50E-06	0.006
ENSG00000175106	TVP23C	Trans-Golgi Network Vesicle Protein 23 Homolog C	17:15502264-15563595	−1.14	4.61E-06	0.006

Author Manuscript

Author Manuscript

Author Manuscript

Author Manuscript

Table 2

GO enrichment analysis for genes differentially expressed between DLB brain tissues and age-matched controls.

ID	Name	p-value	Bonferroni	# Genes
GO:0008366	Axon ensheathment	1.17E-12	3.91E-09	16
GO:0007272	Ensheathment of neurons	1.17E-12	3.91E-09	16
GO:0042552	Myelination	1.23E-11	4.09E-08	15
GO:0048709	Oligodendrocyte differentiation	1.38E-08	4.60E-05	11
GO:0022008	Neurogenesis	2.25E-07	7.48E-04	48
GO:0010001	Glial cell differentiation	2.53E-07	8.41E-04	14
GO:0014003	Oligodendrocyte development	3.07E-07	1.02E-03	7
GO:0014015	Positive regulation of gliogenesis	5.10E-07	1.70E-03	8
GO:0048699	Generation of neurons	8.95E-07	2.98E-03	45
GO:0022010	Central nervous system myelination	9.50E-07	3.16E-03	5
GO:0032291	Axon ensheathment in central nervous system	9.50E-07	3.16E-03	5
GO:0042063	Gliogenesis	1.03E-06	3.43E-03	15
GO:0021782	Glial cell development	1.25E-06	4.16E-03	9
GO:0007417	Central nervous system development	1.51E-06	5.01E-03	30
GO:0050767	Regulation of neurogenesis	5.27E-06	1.76E-02	25
GO:0007422	Peripheral nervous system development	5.37E-06	1.79E-02	8
GO:0014013	Regulation of gliogenesis	5.85E-06	1.95E-02	9
GO:0045687	Positive regulation of glial cell differentiation	6.68E-06	2.22E-02	6
GO:0032989	Cellular component morphogenesis	7.19E-06	2.39E-02	41
GO:0051960	Regulation of nervous system development	1.39E-05	4.62E-02	26